Organomodified Montmorillonite as Filler in Natural and Synthetic Rubber

P. Bala,[1] B. K. Samantaray,[1] S. K. Srivastava,[2] G. B. Nando[3]

[1]*Department of Physics and Meteorology, Indian Institute of Technology, Kharagpur-721302, India*
[2]*Department of Chemistry, Indian Institute of Technology, Kharagpur-721302, India*
[3]*Rubber Technology Centre, Indian Institute of Technology, Kharagpur-721302, India*

Received 7 July 2003; accepted 24 November 2003

ABSTRACT: The filler action of dodecylamine (12C) intercalated montmorillonite (MNT) referred to as organomodified montmorillonite (12C-MNT) up to 4 wt % on natural rubber (NR) and styrene butadiene rubber (SBR) was studied and findings were compared with respect to the unmodified Na-MNT. X-ray analysis was used to calculate the interchain separation (R and R'), degree of crystallinity (X_c), and distortion factor (k). It is noted that R and R' showed the opposite trend, whereas X_c as well as k showed overall increasing trend with an increasing amount of 12C-MNT on both NR and SBR. For Na-MNT (1 wt %) filled NR and SBR, the corresponding magnitude of R and R' and X_c showed nearly no change, whereas k_c increased significantly. The crosslinking density (v_c) does not show any significant changes in NR, whereas for SBR, it increases with increasing 12C-MNT as filler. Interestingly, in the case of 1 wt % pure Na-MNT used as filler for both NR and SBR, v_c was lower compared to the virgin rubbers. Both swelling index (s_i) and sol fraction (Q) do not show any significant variation for NR composites, whereas these decrease for SBR composites with increasing concentration of 12C-MNT filler. On the contrary, NR and SBR with 1 wt % of Na-MNT filler show greater magnitude of s_i and Q corresponding to the pure ones. Measurements of mechanical properties showed a significant increase in tensile strength and elongation at break for NR-12C-MNT (4 wt %) when compared with either virgin NR. In addition, modulus at the elongation at 100 and 200% in general increases with increasing loading of 12C-MNT filler in NR. Similar observations were also noted in the case of SBR. Interestingly, when only pure Na-MNT is used as filler, the strength of NR and SBR decreases drastically. Scanning electron microscopic studies were also to used support the mechanical behavior of NR-12MNT and SBR-12CMNT composites. © 2004 Wiley Periodicals, Inc. J Appl Polym Sci 92: 3583–3592, 2004

Key words: organophilic clay; rubber; X-ray; mechanical properties

INTRODUCTION

In the past, materials with layered structure have received considerable interest mainly because of their interesting physical properties.[1–4] Montmorillonite (MNT) belongs to a smectite group of clay minerals that has 2 : 1 type of layer structure.[4] It consists of negatively charged silica sheets that are held together by charge-balancing counterions such as Mg^{2+}, Na^+, and Ca^{2+}. The general chemical formula of the montmorillonite is $(M_y{}^+.nH_2O)(Al_{4-y}Mg_y)Si_8O_{20}(OH)_4$, where M (M = Na^+, Ca^{2+}, Mg^{2+}, etc.) is the interlayer cation. These interlayer cations balance the negative charges, which are generated by the isomorphous substitution of Mg^{2+} and Fe^{2+} for Al^{3+} in the octahedral sheet and Al^{3+} for Si^{4+} in tetrahedral sheet. Because of the presence of easily exchangeable inorganic cations, organic compounds and polymers could be intercalated into the interlayers of montmorillonite. This results in the expansion of interlayer spacing between the MNT sheets and even may lead to the complete dissociation of the sheets to form MNT–organic composites with a nanometer level.[5–7] These polymer–MNT hybrid materials often show some unexpected improved properties even at a very small fraction of MNT content.[8,9] A nanocomposite of nylon-6 containing only 4 wt % MNT shows significant improvement in the mechanical and thermal properties compared with pure nylon-6.[10] Other polymer–clay nanocomposites based on polypropylene,[11] poly(ethylene oxide),[12] polyaniline,[13] silicone rubber,[14] poly(methyl methacrylate),[15] poly(*N*-vinyl carbazole),[16] polyimide,[17] polyurethane,[18] epoxy resin,[19] ENGAGE rubber,[20] and EVA rubber[21–23] were reported.

To the best of our knowledge, the effect of alkylammonium-intercalated montmorillonite as filler on natural rubber (NR) and styrene butadiene rubber (SBR) has not been reported until now. Hence, in the present investigation, an attempt was made to investigate the effect of alkylammonium-intercalated montmorillonite as filler on NR and SBR and

Correspondence to: S. K. Srivastava (sunit@chem.iitkgp.ernet.in).

Contract grant sponsor: Indian Institute of Technology.
Contract grant sponsor: M.H.R.D.

Journal of Applied Polymer Science, Vol. 92, 3583–3592 (2004)

findings were compared with the pure montmorillonite.

EXPERIMENTAL

Preparation of organophilic montmorillonite

In a 2-L beaker, 40 g of sodium montmorillonite (Na-MNT; Clay Mineral Society, as SW_y1, University of Missouri, Columbia; cation exchange capacity = 76.4 meq/100 g) was dispersed in 1 L hot water at 75°C. A mixture of 17.64 g dodecyl amine (SRL Pvt. Ltd., Mumbai, India), 9.6 mL concentrated hydrochloric acid, and 200 mL distilled water was heated to 80°C. Solution of dodecyl ammonium chloride obtained was added into the dispersion of Na-MNT and was agitated vigorously for about 1 h. The white precipitate thus obtained was filtered, washed with hot water to make it free from chloride ions, and tested by silver nitrate solution. The white product was then dried in a vacuum. The dried product was ground to powder form and sieved by a 270-mesh-sized sieve.

Organophilic clay–rubber composites

NR with grade name ISNR-5 [volatile matter, 1% (max.) by mass; ash, 1% (max.) by mass; initial plasticity, 30 (min.)] used in the present investigation was supplied by Rubber Research Institute of India (Kottayam, India). NR (100 g) and 1 g 12C-MNT were mixed for 15 min at room temperature with 2.5 g sulfur, 5 g ZnO, 2 g stearic acid, 1 g antioxidant, 0.8 g CBS, and 0.2 g TMTD in a roll mill having a speed ratio of 1 (front) : 1.2 (back). The specimens were compression molded in a hydraulically operated press (Moore Press) at 150°C and 5 MPa pressure to obtain the sheets of natural rubber with 1 wt % 12C-MNT. The sheet was termed as NR-12C-MNT (1 wt %). To obtain the NR sheets with 2, 3, and 4 wt % of 12C-MNT, a similar process was followed and the samples were termed as NR-12CMNT (2 wt %), NR-12CMNT (3 wt %), and NR-12CMNT (4 wt %), respectively. To use as reference, NR were vulcanized and compression molded in a same process described above by using 1 wt % Na-MNT as filler [NR-NaMNT (1 wt %)] and without any filler (NRV) but with all the additives used earlier. SBR with grade name SBR1502, supplied by Synthetic and Chemicals Ltd. (Barelley, UP, India), was selected for the present investigation. The process of SBR–montmorillonite compounds was the same as that of natural rubber.

Characterization of the clay–rubber composites

X-ray study

X-ray diffraction patterns of the samples were recorded on a Rigaku Miniflex-diffractometer (30 kV, 10 mA) by using Cu-Kα radiation (λ = 1.5418 Å) with a scanning rate of 2°/min at room temperature. These data were used to calculate degree of crystallinity, distortion parameter, and interchain separations as described as below.

Interchain separation

In the case of the polymer sample, the strong innermost peak is considered to arise from the interatomic vectors between adjacent chains. On the basis of this assumption, the interchain separation can be calculated from the position of the first diffraction maximum by using the equation[24]

$$R = \frac{5}{4}\frac{\lambda}{2\sin\theta} \tag{1}$$

and

$$R' = \frac{7}{2\pi}\frac{\lambda}{2\sin\theta} \tag{2}$$

The interchain separation calculated from eq. (1) is suitable for short-chain polymers, whereas eq. (2) is more suitable for highly oriented amorphous linear polymers.[25]

Degree of crystallinity and distortion

All valid methods of measuring the degree of crystallinity by X-ray diffraction techniques are based on the fact that the total coherent scattering due to N atoms is the same, independent of their state of aggregation.[26,27] Assuming no preferred orientation in the sample, the scattering over the entire reciprocal space can be written as $4\pi\int_0^\infty s^2 I(s)ds$, where s is the magnitude of reciprocal lattice vector given by $s = |s| = (2\sin\theta)/\lambda$, where 2θ is the scattering angle, λ is the wavelength of X-ray radiation, and $I(s)$ represents the intensity of total coherent scattering at the radial distance s in reciprocal space. According to Ruland,[28] if $I(s)$ refers to an intensity scattered from the crystallite phase, then to a first approximation, the weight fraction of the crystalline phase in the specimen is given by

$$X_c = \frac{\int_{s_0}^{s_p} s^2 I_c(s)ds}{\int_{s_0}^{s_p} s^2 I(s)ds} K(s_0, s_p, D, \overline{f^2}) \tag{3}$$

where $\overline{f^2}$ is the mean square atomic scattering factor for the polymer, given by

$$\overline{f^2} = \frac{\Sigma N_i f_i^2}{\Sigma N_i} \tag{4}$$

where N_i is the number of atoms of type I in the empirical formula, D is the lattice imperfection factor, and s_0 and s_p represent the lower and upper limit of integration for the finite and relatively large angular range. The coefficient K allows for the loss in intensity due to lattice imperfection.

Following Vonk,[29] eq. (3) can be written as

$$R(s_p) = \frac{1}{x_c} + \frac{k}{2x_c} s_p^2 \tag{5}$$

where K was approximated as

$$K = 1 + \frac{k}{2} s_p^2 \tag{6}$$

and

$$R(s_p) = \frac{\int_{s_0}^{s_p} Is^2 ds}{\int_{s_0}^{s_p} I_c s^2 ds} \tag{7}$$

Thus, assuming a linear plot of R versus (s_p^2), both degree of crystallinity (X_c) and distortion factor (k) can be obtained from eq. (7).

Measurement of crosslinking density, sol fraction, and swelling index

Crosslinking density, defined as moles of effective network chain per cubic centimeter, was obtained by calculating the volume fraction of the swollen polymer. For this, the NR and SBR slabs were cut into $7 \times 7 \times 2$ mm size and immersed in toluene at 30°C for 24 h. Subsequently, the specimens were removed and weights of the swollen specimens (w_s) were determined after gently wiping off the solvent with coarse filter paper. The weight of the deswollen specimen (w_{ds}) was determined after removing toluene at 100°C for 2 h until constant weights were achieved. From this w_s and w_{ds}, the swell ratio or sol fraction (Q) and swelling index (s_i) are given by

$$Q = \frac{w_s}{w_{ds}} - 1 \tag{8}$$

$$s_i = Q \times 100 \tag{9}$$

The weight fraction of the polymer (w_2) and the solvent (w_1) can then be calculated by the relation

$$w_2 = \frac{1}{1 + Q}$$

and

$$w_1 = 1 - w_2 \tag{10}$$

The volume fraction of the polymer (v_2) in the swollen specimen is given by

$$v_2 = \frac{w_2/e_2}{(w_2/e_2) + (w_1/e_1)} \tag{11}$$

where e_1 and e_2 are the densities of the solvent and the polymer.

From the volume fraction data under equilibrium swollen condition, the crosslink density (v_c) was calculated by the Flory–Rhener equation[30]

$$v_c = \frac{\ln(1 - v_2) + v_2 + v_2^2}{v_s(v_2^{1/3} - v_2/2)} \tag{12}$$

where v_s is the molar volume of the solvent and is 106.3 cm^3 for toluene.[31]

Mechanical properties

Measurements of mechanical properties of the specimens were carried out in a computerized Zwick (model 1445) as per ASTM D 412-80. Tensile strength, elongation at break, and modulus at 100 and 200% elongations were determined.

Scanning electron microprobe studies

A JEOL (JSM-5800) scanning electron microscope (SEM) with an acceleration voltage of 20 kV was used to investigate the fracture surfaces of the samples.

RESULTS AND DISCUSSION

It was observed that the textures as well as homogeneity of the NR-Na-MNT (1 wt %), NR/12C-MNT, SBR-Na-MNT, SBR/12C-MNT composites remained almost unchanged. The color of pure NR and NR-12C-MNT (1 wt %) and NR/12C-MNT (1 and 2 wt %) did not change significantly. However, with increasing filler contents, the color of the resultant composites became somewhat darker with respect to the neat NR as well as for SBR.

X-ray characterization of clay–rubber composites

X-ray diffraction patterns of Na-MMT and organophilic clay (12C-MMT) show a 001 peak at $2\theta = 7.4°$ and $2\theta = 5.6°$ corresponding to an interlayer spacing of 11.94 and 15.78 Å, respectively.[32]

Figure 1 represents X-ray diffractograms of NRV, NR/Na-MNT (1 wt %), and NR/12C-MNT composites with their increasing filler concentration variations. A very faint peak appears almost at the same

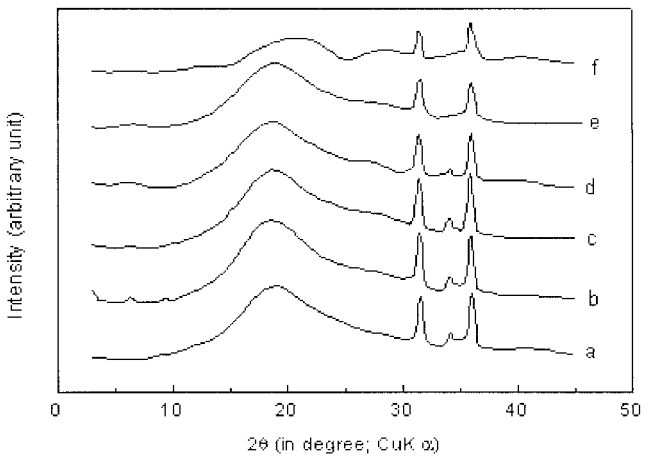

Figure 1 X-ray diffraction (XRD) profiles of NR composites: (a) NRV; (b) NR-NaMNT (1 wt%); (c) NR-12CMNT (1 wt%); (d) NR-12CMNT (2 wt%); (e) NR-12CMNT (3 wt%); (f) NR-12CMNT (4 wt%).

position in all the diffractograms of NR/Na-MNT and NR/12C-MNT composites in Figure 1(b) and (c–f) as observed in the case of pure Na-MNT (d_{001} = 11.94 Å) and organomodified 12C-MNT (d_{001} = 15.78 Å) fillers, respectively. It is also observed that the NRV shows a strong amorphous peak between $2\theta = 5°$ and $2\theta = 30°$ with peak position at $2\theta = 18.81°$. It is observed categorically that the sharpness of all the peaks including the size of the hollow changes with increasing amount of 12C-MNT filler content in NR. This is the conclusive proof for the variation of ordering in NR to which varying amounts of filler have been added. The peak position shifts slightly toward the lower angle region when Na-MNT (1 wt %) as filler is added to NR. In the corresponding composite of NRV with 12C-MNT (1 wt %), the peak position is almost similar to that of the NRV. However, with increasing 12C-MNT filler content, the peak position gradually shifted toward the higher angle region. Interestingly, for NRV, three distinct peaks are observed at 2θ = 31.54, 34.20, and 36.15° with corresponding d values of 2.85, 2.63, and 2.49 Å, respectively. These matched well with that of ZnO,[33] which was added to about 5 wt % in the NRV. The d value of highest intense peak in pure ZnO appears at 2.66 Å. NR and its 12C-MNT composites showed the presence of this peak corresponding to a d value of 2.63 Å and that too of relatively low intensity. This is possibly due to some interactions of ZnO with other additives and rubbers, and finally, changes the preferred orientation. It is interesting to note that the peak corresponding to 2.63 Å almost disappeared when 3 and 4 wt % of 12C-MNT in SBR was used as filler.

The X-ray diffractogram of SBR and its composites are shown in Figure 2. A very broad peak in the range of 2θ = 3–7° appear in both the diffractograms of NR composites with 1 wt % Na-MNT and 12C-MNT [Fig. 2(a, b)]. On the other hand, this broad peak tends to be prominent with increasing organomodified 12C-MNT filler concentration, due to the filler itself, shown in Figure 2(c–f). Interestingly, the peak in the same region of the corresponding composites of NR is relatively of much lower intensity. In addition, a broad peak is also observed at around 19.35°. The addition of 1% Na-MNT to SBR does not show any significant variation of this peak position. It may also be mentioned here that SBRV, similar to NR, shows the presence of the three distinct peaks corresponding to 2.85, 2.64, and 2.50 Å. It is observed that with an increase of 12C-MNT filler, the peak position is shifted toward the lower angle region with decreasing peak intensity. It is also interesting to note that addition of 4 wt % of 12C-MNT filler loading almost diminishes this peak. The comparison of sharpness of peak and size of the hollow indicated that the SBR/12C-MNT composites possess relatively less ordering.

The interchain separations (R and R′) obtained from eqs. (1) and (2) and distance (d) between two crystal surfaces obtained from Bragg's equation for NR and SBR hybrids are shown in Figure 3 and 4, respectively. It is observed from Figure 3 that, in the case of NRV (filler concentration = 0), the value of R and R' are 5.90 and 5.26 Å, respectively, which highly matched the reported value of 5.9 and 5.3 Å.[24] In the case of Na-MNT filler (1 wt %) as filler, the value of R and R' becomes further smaller [i.e., 5.39 and 5.0 Å (Table I)]. The interchain separations of R and R' in NBR and 12C-MNT composites show increasing trend from NRV to NR—1 wt % 12C-MNT. Thereafter, it begins to decline and attains almost the same magnitude as observed in NRV for 2 to 3 wt % of the 12C-MNT/NRV composites. It is subsequently followed by a

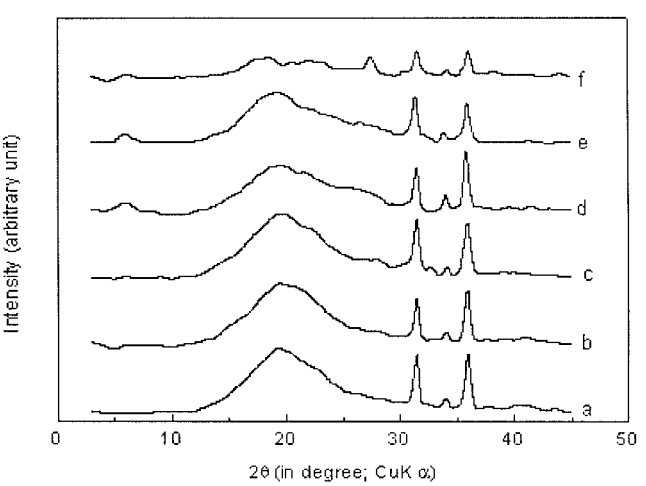

Figure 2 X-ray diffraction profiles of SBR composites: (a) SBRV; (b) SBR-NaMNT (1 wt%); (c) SBR-12CMNT (1 wt%); (d) SBR-12CMNT (2 wt%); (e) SBR-12CMNT (3 wt%); (f) SBR-12CMNT (4 wt%).

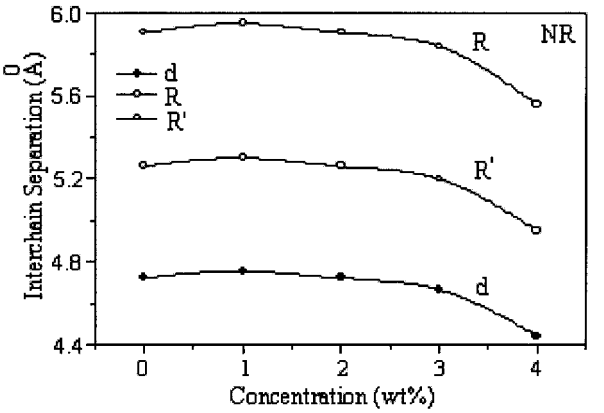

Figure 3 Variation of interchain separation of NR with 12C-MNT filler concentration.

sharp fall in between 3 and 4 wt % of the 12C-MNT/NR composites. Such a behavior is also supported by the X-ray diffraction studies which showed a nearly one-to-one correspondence with R and R' in terms of ordering as mentioned earlier. The interchain separations, R and R', for SBR/1 wt % of Na-MNT are 5.04 Å, 1.25 Å compared to 5.65 Å, 5.08 Å for 1 wt % 12C-MNT/NBR. It is also apparent from Figure 4 that the interchain separation of SBR/1 wt % of 12C-MNT is even lower than that of SBRV. Thereafter, it showed an increasing trend with increasing 12C-MNT filler content.

Table II records the degree of crystallinity (X_c) and distortion factor (k) data deduced from X-ray diffraction studies on NR and SBR with varying amounts of 12C-MNT filler loading. It shows that the magnitude of X_c and k in NRV are 0.38 and 1.00, respectively. The addition of Na-MNT and 12C-MNT (each 1 wt %) in NRV resulted a decrease in X_c, while k becomes more. Interestingly, for 2 to 3 wt % of 12C-MNT, both increased continuously and became steady for 4 wt % of 12C-MNT. It may be interesting to mention that the

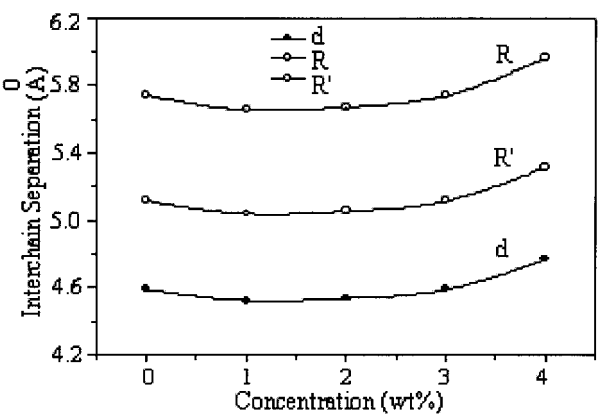

Figure 4 Variation of interchain separation of SBR with 12C-MNT filler concentration.

maximum value of k observed for 4 wt % 12C-MNT filler (i.e., 2.40) is considerably smaller than that of the 1 wt % of Na-MNT (i.e., 3.65. X_c and k shows no significant change in for 1 wt % of Na-MNT and 12C-MNT or 2 wt % of 12C-MNT SBR composites). However, a sharp decrease in X_c and increase in k is reflected for 3 and 4 wt % 12C-MNT/SBR composites. It is also observed that similar to natural rubber, k is increased when pure Na-MNT acts as filler in SBR. The variation of k is not so significant as the amount of 12C-MNT filler in SBR is increased.

In general, it can be concluded from X-ray data that the distortion factor k increases with increasing filler content in both NR and SBR composites, indicating more and more disorder. However, the trend of variation of degree of crystallinity (X_c) in both NR and SBR composites are of opposite type (i.e., it increases in NR/12C-MNT, whereas it decreases for SBR/12C-MNT with increasing filler concentration). One can consider that the contribution to disorder parameter k is because of the contribution from two factors, namely, from the crystallites and from its intercrystalline regions. Whenever the disorder in crystalline region falls, there is an increase in the crystallinity. That is the case with SBR composites. On the other hand, when the disorder in the crystalline regions increases, the crystallinity falls, as in the case of NR composites. The results show that there is an overall increase in the value of k, which is because of greater contributions from the intercrystalline regions.

Crosslinking density, sol fraction, and swelling index

Table II also presents the data related to the crosslinking density (v_c), swelling index (s_i), and solfraction (Q) for NR and SBR composites with 12C-MNT filler loading. It is seen that the crosslinking density, v_c, does not show any significant changes with respect to concentration of 12C-MNT filler in NR. In the case of SBR, it increased up to 3 wt % and beyond this concentration it becomes almost steady. It may be interesting to note that both NR and SBR with 1 wt % pure Na-MNT filler show the crosslinking density to be lower than compound without filler. The variation of swelling index

TABLE I
Properties of NR and SBR with 1 wt % NaMNT Filler

Characteristic/properties	NR-NaMNT (1 wt %)	SBR-NaMNT (1 wt %)
Interchain separation (R)	5.39	5.04
Interchain separation (R')	5.0	1.25
Tensile strength (TS) [MPa]	342	210
Elongation at break (EB)	0.78	0.76
Modulus at 100% elongation[a]	1.50	1.17
Modulus at 200% elongation[a]	6.05	5.67

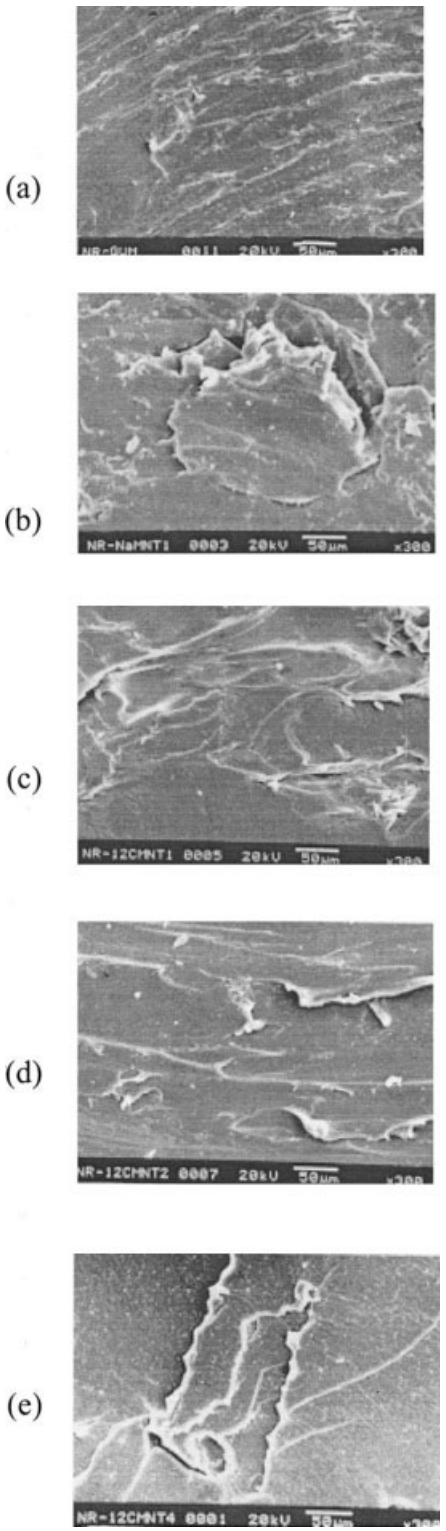

Figure 5 SEM micrographs (a) NRV, (b) NR-NaMNT (1 wt %), (c) NR-12C-MNT (1 wt %), (d) NR-12CMNT (2 wt %), (e) NR-12CMNT (4 wt %).

(s_i) and solfraction (Q) with 12C-MNT concentration showed that both s_i and Q decrease with increasing concentration of 12C-MNT filler in SBR. It is also seen that the rate of decrease of s_i and Q occurs rapidly up to 3 wt % of filler. Thereafter, no significant variation in either s_i or Q is noted. It is also interesting to mention here that NR composites do not show any significant variation in s_i and Q with 12C-MNT filler. On the contrary, NR and SBR with 1 wt % of Na-MNT

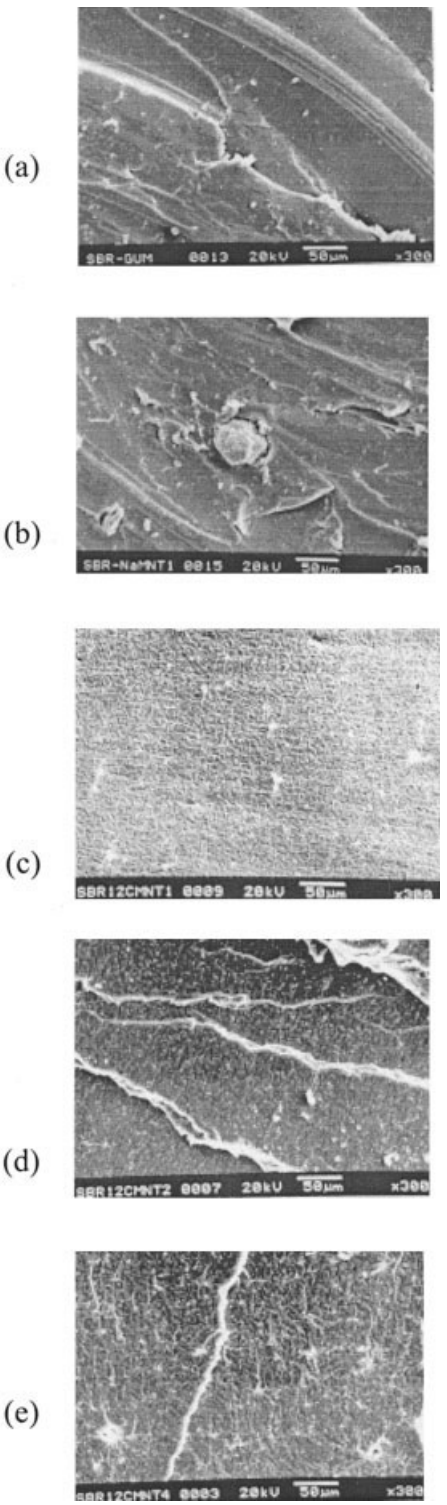

Figure 6 SEM micrographs (a) SBRV, (b) SBR-NaMNT (1 wt %), (c) SBR-12CMNT (1 wt %), (d) SBR-12CMNT (2 wt %), (e) SBR-12CMNT (4 wt %).

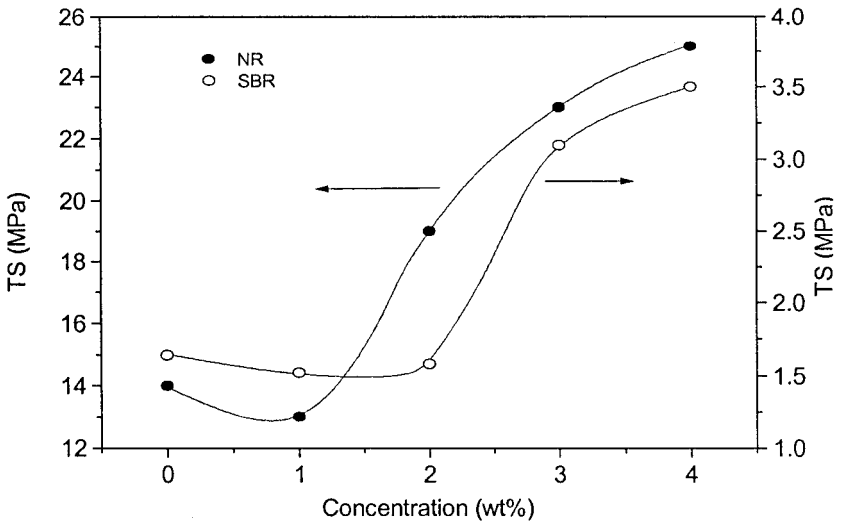

Figure 7 Variations of tensile strength (TS) as a function of 12C-MNT filler concentration in NR and SBR.

filler shows greater magnitude of s_i and Q corresponding to the pure ones.

It is well known that filler rubber interaction resists solvent swelling of the composites. As observed in cases of NR and SBR, interaction of 12C-MNT enhances the physical properties of the composites through reduction of aggregation size or increase in effective surface for interaction with polymer. Thus, it is expected that gradual loading of filler (12C-MNT) would decrease solvent swelling and that is the case with SBR composites. However, the swelling behavior of NR/12C-MNT composites does not change significantly with varying 12C-MNT filler loading. It is anticipated that the intercalated clay, 12C-MNT, consists of a long dodecyl aliphatic chain, which has well dispersed into NR. However, the possibility of intercalation of NR chain into interlayer spaces of montmorillonite cannot be completely ruled out. Because of the possibility of strong interaction of these dodecyl chains in NR, solvent appears to be incapable of penetrating the NR/12C-MNT matrix up to 3 wt % 12C-MNT filer. Thereafter, the solvent is in a position to penetrate and counterbalances the effect of filler–rubber interaction.

Scanning electron microscopy analysis

Figures 5(a) and 6(a) represent the SEM micrographs of the fracture surface of NR and SBR, respectively. It is observed that when pure Na-MNT is used as filler in NR the size of the aggregation of Na-MNT in polymer matrix is well visualized [Fig. 5(b)]. Therefore, it may be inferred that the pure Na-MNT is not compatible with NR and creates a phase separation showing thereby a larger aggregation of montmorillonite particles. In the case of intercalated montmorillonite (12C-MNT), however, the aggregation of alkylammonium-intercalated montmorillonite particles disappeared [Fig. 5(c); i.e., 12C-MNT constitutes relatively much more compatibly to NR system]. This in turn enhances the dispersion of 12-MMT into the polymer matrix. It is observed that SBR also shows almost similar type of behavior. The dispersion of 12C-MNT particles do not reach the same level as that of NR (Fig. 5). Possibly the intercalated montmorillonite with dodecyl long aliphatic chain is not compatible with aromatic styrene–butadiene rubber. As a result, the interaction of SBR does not occur to that extent of NR, which causes the poorer dispersion of 12C-MNT in SBR compared to NR.

Mechanical properties of clay–rubber composites

The variation of tensile strength (TS) of NR and SBR with changes of concentration of dodecyl alkylammonium filler is shown in Figure 7. It is observed that the TS of the NR and SBR with 1 wt % 12C-MNT filler is almost the same as that of vulcanized NR and SBR without any filler. The TS of NR with 1 wt % of Na-MNT filler decreased approximately to 30% that of NR (Table I). In the case of SBR, this type of decrease is also observed when pure Na-MNT filler is used. It is also noted that TS of NR and SBR increases with an increase of 12C-MNT filler content and it becomes maximum at 4 wt %.

Figure 8 represents the variation of elongation at break with respect to concentration of 12C-MNT filler for NR and SBR composites. The elongation at break (EB) of the NR with 1 wt % 12C-MNT shows a lower value as compared with NRV. It shows, however, an increasing trend with an increase of 12C-MNT filler content and maximum value obtained for 4 wt % of

TABLE II
Crystallinity (X_C), Distortion Parameter (k), and Crosslinking Density (v_C), Swelling Index (Si), and Solfraction (Q) Data for NR, SBR, and Its 12C-MNT Composites

Samples	X_c	k	v_c (mol/mL)	s_c	Q
NRV	0.38	1.00	3.90×10^{-4}	316	3.18
NR-12CMNT (1 wt %)	0.34	1.51	3.80×10^{-4}	322	3.26
NR-12CMNT (2 wt %)	0.37	1.73	3.76×10^{-4}	330	3.30
NR-12CMNT (3 wt %)	0.47	1.96	3.73×10^{-4}	338	3.36
NR-12CMNT (4 wt %)	0.48	2.40	3.85×10^{-4}	335	3.36
SBRV	1.62	0.32	3.56×10^{-4}	310	3.13
SBR-12CMNT (1 wt %)	1.64	0.31	4.03×10^{-4}	310	3.09
SBR-12CMNT (2 wt %)	1.43	0.29	5.25×10^{-4}	260	2.59
SBR-12CMNT (3 wt %)	1.46	0.37	5.80×10^{-4}	235	2.42
SBR-12CMNT (4 wt %)	1.35	0.52	5.78×10^{-4}	233	2.33

12C-MNT in the present investigation, which is considerably greater than that of NRV (Table I). It is interesting to note that this parameter decreased drastically when compared to NR with only 1 wt % of Na-MNT. In the case of SBR with 12C-MNT filler, the trend of variation of EB with concentration is nearly same as that of NR. In the case of SBR with 1 wt % of Na-MNT filler, the fall is not so drastic.

Figure 9 shows the variation of modulus of NR at elongation at 100 and 200% with respect to concentration of 12C-MNT filler. It is observed that these moduli for 1 wt % 12C-MNT content show nearly same value from that of NR without any filler, but these moduli increase with an increase of filler content and become almost steady after 2 wt %. The value of modulus at elongation at 100% for 1 wt % of Na-MNT content is nearly same as that of NRV and that of 1 wt % of 12C-MNT, but for 200%, it is smaller than the respective value of 12C-MNT filler. The variation of modulus of SBR at elongation at 100 and 200% is shown in Figure 10. It is observed that these moduli for SBR with 1 wt % 12C-MNT filler is almost the same as that of SBR without any filler. It is also observed that these moduli increase with an increase of concentration of 12C-MNT filler and these become maximum at 2 wt % of 12C-MNT filler; beyond this, these become almost steady. It is interesting to note that SBR with 1 wt % of Na-MNT filler shows a lower value as compared with SBR without any filler.

The improvements of tensile strength and tensile modulus in the case of polymer–clay hybrid and nanocomposites are given by some researchers.[34,35] Their studies suggest that the increase of strength and modulus is related to the degree of dispersion of clay layers into the polymer matrix. Some explanations are present on the basis of interfacial properties and restricted mobility of the polymer chain.[36] According to the Usuki et al.,[37] strong ionic interaction between polymers and silicate layers, which generates some crystallinity at the interface, is responsible for reinforcement effect. It seems that the explanation or modeling of the increase of TS and elongation at break for

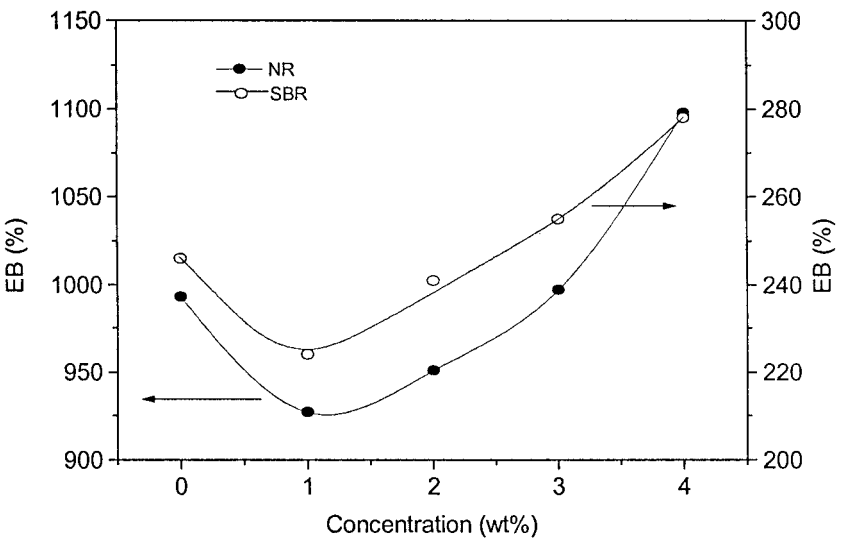

Figure 8 Variations of elongation at break (EB) as a function of 12C-MNT filler concentration in NR and SBR.

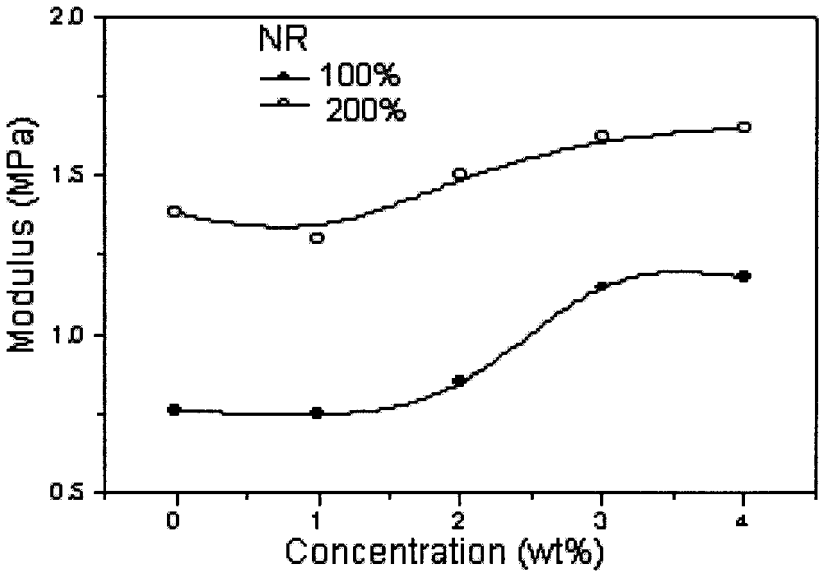

Figure 9 Variations of modulus of NR as a function of 12C-MNT filler concentration.

the NR–intercalated clay hybrid materials is not straightforward. Any comparison of modeling results with experimental data would be further complicated by the fact that particle aggregation influences the TS, EB, and modulus of the composite. Pure montmorillonite sample is hydrophilic in nature but, when it is intercalated with dodecyl ammonium, it becomes organophilic, which has a high tendency to be compatible with the polymeric system.[38–40] It is observed from Figure 5(b) that Na-MNT did not disperse well into the polymer matrix, which caused the aggregation of Na-MNT particles, whereas in Figure 5(c, d), the aggregation of the 12C-MNT particles disappear. Thus, in the present investigation, it appears that pure Na-MNT becomes incompatible to the NR system, so the particle aggregation of the montmorillonite becomes larger, which gives a very low value of TS and EB of NR-NaMNT (1 wt %) compounds, whereas the intercalated montmorillonite (12C-MNT) becomes compatible and expected some filler–rubber interactions, which causes the dispersion of the 12C-MNT particles within the polymer matrix. It is also observed in the present investigation that crystallinity increases significantly with incorporation of 12C-MNT filler. Thus, it appears that the improvements of tensile properties are due to the good dispersion of 12C-MNT into polymer matrix and an ionic or van der Waals type interaction takes place between the rubber chain and silicate layers, which developed some crystallinity in the sample, and finally, enhanced the mechanical

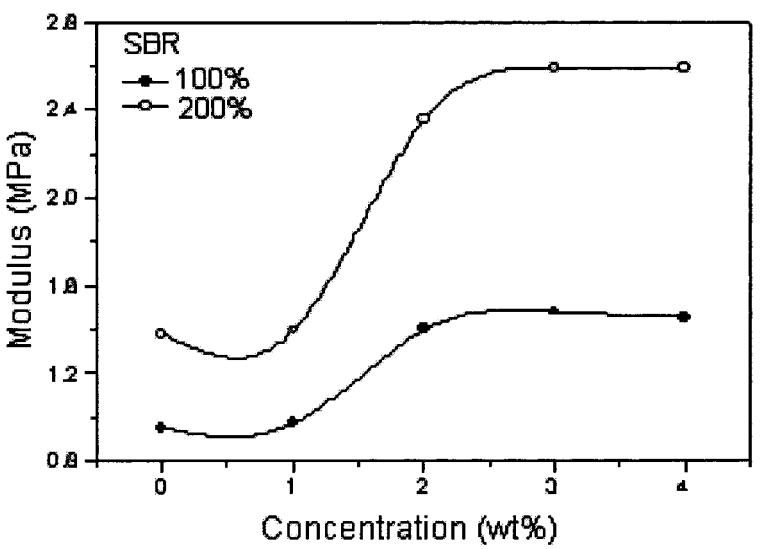

Figure 10. Variations of modulus of SBR as a function of 12C-MNT filler concentration.

properties of NR. In the case of SBR, we also observed the same type of trend of the variation of TS, EB, and modulus with that of NR compounds, which also supports the finding that reinforcement taking place in the present case is mainly due to some sort of surface interaction of montmorillonite layers with polymer chain.

CONCLUSION

The filler effects of organomodified dodecyl alkylammonium intercalated montmorillonite (12C-MNT) were investigated for NR and SBR. X-ray analysis showed that the variation of interchain separations, R and R', and degree of crystallinity, X_c, for 12C-MNT composites of NR are just opposite to the corresponding SBR composites. However, the distortion factor, k, showed an increasing trend with increasing 12C-MNT filler contents. The crosslinking density (v_c), swelling index (s_i), and sol fraction (Q) do not show any significant changes in NR, while for SBR, v_c increases and s_i and Q decrease with 12C-MNT. All these parameters (i.e., R and R', X_c, k, v_c, s_i, and Q) for organomodified 1 wt % of 12C-MNT were compared with that of unmodified 1 wt % of Na-MNT. Tensile strength, modulus, and elongation at break increased significantly as compared to pure vulcanized NR and SBR when 4 wt % of 12C-MNT was used as filler. In the case of NR, these properties decreased drastically for 1 wt % of pure Na-MNT. SEM studies were also made on the fractured surfaces of these samples and correlated with the above properties.

The authors acknowledge the assistance provided by the Institute and M.H.R.D.

References

1. Lieth, R. M. A. Preparation and Crystal Growth of Materials with Layered Structures; Reidel: Dordrecht, 1977.
2. Haeuseler, H.; Srivastava, S. K. Z Kristallogr 2000, 215, 205.
3. Srivastava, S. K.; Pramanik, M.; Palit, D.; Mathur, B. K.; Samantaray, B. K.; Haeuseler, H. Chem Mater 2001, 13, 4342.
4. Crystal Structure of Clay Minerals and X-ray Identification; Brindley, G. W., Brown, G., Eds.; Mineralogical Society: London, 1980.
5. Kornmann, X.; Berglund, L. A.; Sterte, J.; Giannelis, E. P. Polym Eng Sci 1998, 36, 135.
6. Wang, Y.; Zhang, L.; Tang, C.; Yu, D. J Appl Polym Sci 2000, 78, 1879.
7. Fu, X.; Qutubuddin, S. Mater Lett 2000, 42, 12.
8. Huang, J.; Zhu, Z.; Ma, X.; Qian, X.; Yin, J. J Mater Sci 2000, 36, 871.
9. Chen, G.; Kawasumi, M.; Kato, A.; Usuki, A.; Okada, A. J Appl Polym Sci 1999, 73, 425.
10. Kojima, Y.; Usuki, A.; Kawasumi, M.; Okada, A.; Kurauchi, T.; Kamigito, O. J Polym Sci, Part A: Polym Chem 1993, 31, 1755.
11. Kawasumi, M.; Hasegawa, N.; Kato, M.; Usuki, A.; Okada, A. Macromolecules 1999, 30, 6333.
12. Vaia, R. A.; Sauer, B. B.; Tse, O. K.; Giannelis, E. P. J Polym Sci, Part B: Polym Phys 1997, 35, 59.
13. Biswas, M.; Sinha Roy, S. J Appl Polym Sci 2000, 77, 2948.
14. Wang, S.; Lang, C.; Wang, X.; Li, Q.; Qi, Z. J Appl Polym Sci 1998, 69, 1557.
15. Lee, D. C.; Lee, W. J. J Appl Polym Sci 1996, 61, 1117.
16. Biswas, M.; Sinha Roy, S. Polymer 1998, 39, 6423.
17. Delozier, D. M.; Orwoll, R. A.; Cahoon, J. F.; Johnstom, N. J., Jr.; Connell, J. W. Polymer 2002, 43, 813.
18. Wang, Z.; Pinnavaia, T. J. Chem Mater 1998, 10, 3769.
19. Ke, Y.; Lu, J.; Yi, J. X.; Zhao, J.; Qi, Z. J Appl Polym Sci 2000, 78, 808.
20. Ray, S.; Bhowmick, A. K. Rubber Chem Technol 2002, 74, 835.
21. Pramanik, M.; Srivastava, S. K.; Samantaray, B. K.; Bhowmick, A. K. J Appl Polym Sci 2003, 87, 2216.
22. Pramanik, M.; Srivastava, S. K.; Samantaray, B. K.; Bhowmick, A. K. J Polym Sci, Part B: Polym Phys 2002, 40, 2065.
23. Pramanik, M.; Srivastava, S. K.; Samantaray, B. K.; Bhowmick, A. K. Macromol Res 2003, 11, 260.
24. Jia, W.; Segal, E.; Kornemandel, D.; Lamhot, Y.; Narkis, M.; Siegmann, A. Synth Met 2002, 128, 115.
25. Klug, H. P.; Alexander, L. E. X-ray Diffraction Procedures; Wiley-Interscience: New York, 1974; Chapter 12.
26. L. E. Alexander, X-ray Diffraction Methods in Polymer Science; Wiley-Interscience: New York, 1969.
27. Spruiell, J. E.; Clark, E. S. Methods of Experimental Physics, Part B; Fara, R. A., Ed.; Academic Press: San Diego, 1980; Vol. 16, p 99.
28. Ruland, W. Acta Crystallogr 1961, 14, 1180.
29. Vonk, C. G. J Appl Crystallogr 1973, 6, 148.
30. Flory, P. J. Principles of Polymer Chemistry; Cornell Univ. Press: Ithaca, NY, 1953; p 579.
31. Jain, S. R.; Sekkar, V.; Krishnamurthy, V. N. J Appl Polym Sci 1993, 48, 1515.
32. Pramanik, M.; Srivastava, S. K.; Samantaray, B. K.; Bhowmick, A. K. J Mater Sci Lett 2001, 20, 1717.
33. Powder diffraction file no. 21-1486, JCPDS, Intl. Centre for Diffraction Data, U.S.A.
34. Shi, H.; Lan, T.; Pinnavaia, T. J. Chem Mater 1996, 8, 1584.
35. Shia, D.; Hui, C. Y.; Burnside, S. D.; Giannelis, E. P. Polym Comp 1998, 19, 608.
36. Massam, J.; Pinnavaia, T. J. Mater Res Soc Symp Proc 1998, 520, 223.
37. Usuki, A.; Koiwai, A.; Kojima, Y.; Kawassumi, M.; Okada, A.; Kurauchi, T.; Kamigaito, O. J Appl Polym Sci 1995, 55, 119.
38. Usuki, A.; Kojima, Y.; Kawasumi, M.; Okada, A.; Fukushima, Y.; Kurauchi, T.; Kamigato, O. J Mater Res 1993, 8, 1185.
39. Kojima, Y.; Fukumori, K.; Usuki, A.; Okada, A.; Kurauchi, T. J Mater Sci Lett 1993, 12, 889.
40. Kojima, Y.; Usuki, A.; Kawasumi, M.; Okada, A.; Kurauchi, T.; Kamigaito, O. J. J Polym Sci, Part A: Polym Chem 1993, 31 1755.